

Optimizing Uncertainty-Aware Deep Learning for On-the-Edge Murmur Detection in Low-Resource Settings

Andrea De Simone, Noemi Giordano, Silvia Seoni, Kristen M. Meiburger, and Fabrizio Riente

Abstract—Early and reliable detection of heart murmurs is essential for the timely diagnosis of cardiovascular diseases, yet traditional auscultation remains subjective and dependent on expert interpretation. This work investigates artificial intelligence (AI)-based murmur detection using the CirCor Heart Sound dataset, with a focus on enabling uncertainty-aware, resource-efficient deployment on edge devices. Three convolutional neural network (CNN) architectures of increasing complexity (Light, Baseline, and Heavy) were compared in terms of classification performance, computational cost, and suitability for on-device inference. Additionally, Monte Carlo Dropout was applied for uncertainty estimation, providing confidence measures to improve prediction sensitivity. Results show that lightweight models can achieve accuracy comparable to deeper networks ($\sim 91\%$) while requiring two orders of magnitude fewer parameters. Incorporating uncertainty-based selective classification further improved sensitivity by 3%, enhancing robustness and clinical reliability. The findings highlight the feasibility of developing computationally efficient, uncertainty-aware AI systems for heart murmur screening in low-resource and remote healthcare settings.

Index Terms—heart sound analysis, edge computing, uncertainty quantification, medical signal processing

I. INTRODUCTION

CARDIOVASCULAR diseases (CVDs) confirmed to be the leading cause of death worldwide in the current millennium [1]. The prevalence of CVDs is rising also in low-middle income countries, raising the interest of the scientific community in cost-effective CVD screening methods [2]. Digital auscultation can be an interesting candidate, particularly in low-resource scenarios, where access to advanced diagnostic equipment and specialized clinical staff is typically limited. Heart sound recording technology is portable and low-cost: unlike image-based diagnostic technology, such as echocardiography or cardiac computed tomography, electronic stethoscopes can be easily integrated into primary care or even

A. De Simone and F. Riente are with the QNANO group, Department of Electronics and Telecommunications, Politecnico di Torino, Torino, Italy (e-mail: andrea.desimone@polito.it, fabrizio.riente@polito.it).

N. Giordano is with the Department of Health Science and Technology, Aalborg University, Aalborg, Denmark (e-mail: nogi@hst.aau.dk).

S. Seoni and K.M. Meiburger are with the Biolab, Polito ^{BIO}Med Lab, Department of Electronics and Telecommunications, Politecnico di Torino, Torino, Italy. (e-mail: silvia.seoni@polito.it, kristen.meiburger@polito.it).

community or domiciliary settings.

In particular, the presence of heart murmurs has previously been proven to be an effective biomarker for the detection of Congenital Heart Diseases (CHD), which play an important role in pediatric healthcare [3]–[5]. Murmurs are generated by turbulent flow within the heart chambers or large vessels which often arise as a consequence of structural abnormalities such as septal defects, stenosis, or regurgitations [6].

The potentiality of heart murmurs analysis for CHD screening in low-resource scenario resulted, in 2022, in the release of the CirCor Digiscope dataset [7]. CirCor is currently the largest publicly available dataset of pediatric heart sound recordings, acquired in low-resource settings in rural Brazil [8]. The dataset includes recordings performed in real-life scenarios: noise, low-quality signals, and label uncertainty make the dataset a benchmark for the development of murmurs detection methods that could be deployed in real low-resource scenarios. Murmur detection on CirCor was the object of the George B. Moody PhysioNet Challenge 2022 [9], stimulating the design of a high number of data-driven approaches for heart murmurs detection and classification. Even if previous works achieved good performance in the detection task, existing literature mostly overlooked two strategical aspects for the deployment of the detectors in a real low-resource scenario. On one side, the availability of high-resource or cloud computing cannot be taken for granted in these settings due to the lack of internet connection and the unavailability of powerful computers [10], [11]. Therefore, low-resource methods that can be deployed on the edge (on board the recording device itself) should be considered a preferable choice [12]. On the other side, AI-based diagnostic systems inherently suffer from their black-box nature, which prevents users from understanding how predictions are generated and how reliable they are. Moreover, deep learning models are often miscalibrated, showing high confidence on incorrect or out-of-distribution samples, thus limiting their generalization and clinical trustworthiness [13]. To address these issues, Uncertainty Quantification (UQ) techniques have been introduced to provide a numerical estimate of prediction reliability [14]. UQ can support model calibration [15] and enable selective classification [16], where uncertain samples are flagged or discarded, leading to safer and more robust decision-making. Integrating UQ into murmur detection systems can enhance clinical applicability by identifying unreliable predictions and assessing model behavior on ambiguous

or unclassifiable recordings.

In this context, the goal of this work is to propose an AI-based approach for heart murmurs detection in heart sounds in a low-resource scenario with a focus on:

- Objective 1: the comparison of solutions with different computational cost, with the aim of providing a performative yet cost-effective solution that can be, in the future, implemented on the edge.
- Objective 2: the use of an uncertainty analysis aimed at providing the user with a confidence score regarding the murmur detector to enable selective classification.

The rest of the manuscript is organized as follows.

Section II provides an overview of existing methods, with a focus on lightweight classifiers and UQ applied on the task of interest. Section III presents our proposed approach, with details about the feature extraction phase, the model and the methods for UQ; results are showcased in Section IV. In Section V we will discuss the advances with respect to the state of the art, with a focus on the trade-off between detection accuracy and computational cost and on the role of UQ. Finally, we discuss the current limitations as well as the potential future directions.

II. BACKGROUND

A. Heart murmur detectors

A large number of works previously tackled the problem of detecting heart murmurs on the CirCor dataset, stimulated, in the first place, by the George B. Moody PhysioNet Challenge 2022 [9]. Among the winners, the CUED Acoustics team proposed a hybrid recurrent neural network with Gate Recurrent Unit (GRU) and hidden semi-Markov model (HSMM) algorithm that can both segment the signal and detect a heart murmur [17]. This first stage receives as input the spectrogram of the recording and produces four segmentations using four parallel HSMMs. Finally, the confidence of the parallel segmentation is compared to infer the most probable segmentation, murmur prediction, and estimate on the signal quality [17]. HearTech+ was a co-winner of the Challenge [18]. Their system employs a Hierarchical Multi-Scale Convolutional Network (HMS-Net) to perform both murmur detection and clinical-outcome classification. During the challenge as well as later on, most previous works preferred DL approaches over Machine Learning (ML) [19], mainly due to the inherent difficulty in handcrafting relevant features from sounds. The use of DL shifted the focus from computationally expensive signal segmentation steps towards the representation of the signal in different domains.

The proposed input representations can be classified into two families: A) time-frequency representation, including Short-Time Fourier Transform (STFT) [20]–[26] and Continuous Wavelet Transform (CWT) [20], [27]; and B) spectral features, such as Mel Frequency Cepstral Coefficients (MFCCs) [22], [24], [28]–[30] and Mel Spectrogram [26], [31]. Few previous works achieved good performances by applying DL directly on the signal (or sub-segments) in the time domain [32], [33]. Concerning the selection of the DL model, most previous

works aiming at keeping the computational cost to reasonable levels relied on Convolutional Neural Networks (CNN), either pure [26], [28], [32] or combined with recurrent layers [21], attention layers [29] or LSTM [20]. Other successful approaches include Recurrent Neural Networks (RNN) [25] and transformers [34].

B. Challenges and motivation for on the edge computing

As shown, most detectors today rely on DL models, whose complexity may vary quite significantly depending on the architecture: implementation on the edge may be challenging if not designed from the beginning. In this scenario, few state of the art works focused on the deployability of their proposed heart murmurs detectors on microcontroller-based embedded systems. Safdar et al. made the greatest reported effort in this sense, and tested their highly accurate transformer-based detector both on high performance computers and on embedded systems (Raspberry Pi 4), with an inference time of respectively 6.5 and 120 milliseconds for a single audio segment [28]. Morshed et al. reported for their CNN-based detector a time of inference as low as 4 to 10 milliseconds on Google Colab Pro cloud [32]. Similarly, Suma et al. report an inference time of 17 milliseconds on a Tesla T4 GPU, but do not report testing on microcontroller units (MCU) [35]. Kalimuthu et al. report inference times between 16 and 241 milliseconds for various ML and DL methods [29], but do not provide any information on the testing environment. Other previous works describe potentially lightweight approaches, but do not report results concerning testing on embedding systems [20], [25], [34], [36]–[38], considering that in most cases the models will not fit in a resource constrained MCU. This work targets the current gap in validated edge-based heart-murmur detectors by proposing lightweight models tailored for resource-limited microcontrollers. The study highlights the accuracy–complexity trade-off and shows that uncertainty quantification can improve the sensitivity of low-cost implementations.

C. Uncertainty quantification in AI-based methods

Only a few previous works explored the use of UQ for the task of interest. Two participants to the Challenge embedded UQ in their models with the goal of screening out unknown samples, i.e. recordings the expert annotator was not able to classify [39], [40]. Later, Zhang et al. leveraged UQ for the purposes of model calibration, by applying Monte Carlo Dropout (MCD) and temperature scaling, demonstrating a reduction of the Expected Calibration Error of 50% [41]. Elola et al. proposed the use of UQ for a post-hoc analysis of their performances, showing that the uncertainty estimate was consistently higher for miss-classified patients [42].

In this work, our goal is to leverage UQ to especially enhance the system’s sensitivity (or recall) when used by inexperienced users in low-resource scenarios. In this context, advancing from the state of the art, we test the potentiality of UQ using MCD for establishing a confidence score of the models’ prediction to enhance classification and differentiate between *known* and *unknown* recordings.

III. MATERIALS AND METHODS

A. Description of the dataset

The CirCor DigiScope Phonocardiogram Dataset [7], contains a large number of pediatric heart-sound recordings collected during two mass-screening campaigns in Brazil in 2014 and 2015. The dataset contains 5272 phonocardiogram (PCG) recordings from 1568 subjects (mean age 6.1 ± 4.3 years; range 0 – 21 years). All PCGs have been recorded using the Littmann 3200 electronic stethoscope. Individual recordings last 4.8–80.4 s (mean 22.9 ± 7.4 s), with more than 33.5 h of audio. Multiple recordings per subject are available from the standard auscultation sites (aortic, pulmonic, tricuspid and mitral). The dataset contains a subject description file and segmentation file for every recording, containing segmentation information regarding the start and end points of the fundamental heart sounds S1 and S2. The CirCor aimed to support research on murmur detection. Indeed, every audio recording is annotated with three possible labels: murmur absent, murmur present or unknown. Recordings marked as unknown by the annotator represent signal that did not meet the required signal quality standards, i.e. recordings did not lead to a reliable murmur characterization and description. The entire dataset is partitioned into training (60%), validation

TABLE I: Distribution of murmur labels across dataset splits. Entries are recordings with unique patients in parentheses.

	Absent	Present	Unknown
Train	2508 (695)	499 (179)	156 (68)
Validation	308 (106)	69 (27)	37 (16)
Test	1249 (343)	289 (99)	85 (35)

(30%) and test sets (10%). Table I summarizes the label distribution for the three murmur classes (Absent, Present, Unknown) across the train/validation/test splits. Counts refer to recordings, with the corresponding number of unique patients shown in parentheses. The dataset is markedly imbalanced. In total, Absent accounts for 4065/5200 recordings (78.2%), Present for 857/5200 (16.5%), and Unknown for 278/5200 (5.3%). Patient counts sum to 1568 (1144 Absent, 305 Present, 119 Unknown), confirming that multiple recordings per patient are available. This imbalance motivated us to approach the problem in a different way from previous studies, reformulating the classification problem to improve the model performance by maintaining a low level of parameters.

B. Feature extraction

Frequency-domain features were extracted from the raw audio signals using the STFT. This technique computes the Fast Fourier Transform (FFT) over short, overlapping segments of the signal, after multiplying each segment by a windowing function to reduce spectral leakage. In this work, a Hann window was employed, which is commonly used for this purpose. The segment length, denoted as N_{FFT} , is typically chosen as a power of two to improve computational efficiency. The STFT produces a two-dimensional matrix, where the first dimension represents the number of positive frequency bins ($N_{FFT}/2 + 1$) and the second dimension corresponds

to the time windows. To focus on the clinically relevant frequency range, only the lower half of the frequency bins were retained, effectively applying a low-pass filter with a cutoff at 1 kHz, as higher frequencies generally do not contain meaningful heart sound information [18]. Rather than applying STFT to the entire audio recording at once, the signal was further segmented into 2-second windows with a 1-second overlap. This choice ensures that each segment captures at least one complete systolic-diastolic cardiac cycle. As a result, for each patient and recording location, the feature extraction process generates a series of two-dimensional spectrograms, the number of which depends on the duration of the original recording.

C. Model architectures & training details

A CNN model was developed to detect the presence of cardiac murmurs using the previously extracted 2D features. Due to significant class imbalance and variations in audio quality, several design decisions were implemented to improve model performance, as outlined in Fig. 1. First of all, patients labeled

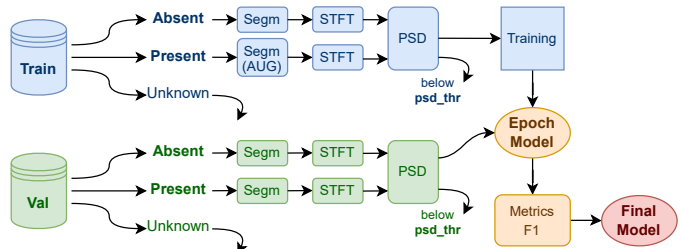


Fig. 1: Representation of the feature extraction and training pipeline. Raw audio is segmented (samples labeled *Present* are augmented through oversampling), and STFT are computed.

as *Unknown* were excluded from the training set. This decision was motivated by the limited number of such cases and the difficulty in distinguishing them from *Known* samples (i.e., those labeled *Absent* or *Present*). The *Unknown* label typically arises from poor audio quality or the presence of confounding conditions that prevent expert annotation. Since the primary goal of this work is to accurately detect murmur presence, the problem was reformulated as a binary classification task (*Absent* vs. *Present*). To address the imbalance between the two classes, the number of features in the *Present* class was artificially increased through oversampling. Specifically, the 1-second step used during segmentation was divided by four, thereby generating additional overlapping segments and approximately balancing the class distributions.

Following feature extraction, each segment underwent a quality assessment based on its power spectral density (PSD). The PSD is computed for each segment over two frequency bands: 20–200 Hz and 0–1000 Hz, as shown in Eq. 1. Here X denotes the STFT matrix, while b_x , b_y and b_n present the frequency bins corresponding to 20 Hz, 200 Hz, and 1000 Hz, respectively. T denotes the last short-time segment.

$$PSD_{\text{band}} = \sum_{b=b_x}^{b_y} \sum_{t=0}^T |X_{b,t}|^2, \quad PSD_{\text{tot}} = \sum_{b=0}^{b_n} \sum_{t=0}^T |X_{b,t}|^2. \quad (1)$$

Finally, the ratio is calculated as $PSD_{ratio} = P_{band}/P_{tot}$. The 20–200 Hz frequency range was selected since the systolic and diastolic components of heart sounds exhibit the highest energy within this band. Segments with a PSD_{ratio} below a predefined threshold "psd.thr" were considered low-quality and discarded. To ensure that data from each recording location remained available, at least the five highest-quality segments per location were retained, even if their PSD values were below the threshold.

Three CNN variants, named **Light**, **Baseline**, and **Heavy**, were

TABLE II: The Architecture of the Three Proposed Models

LIGHT				
Layer	In CH	Out CH	Activation	Dropout
Conv2d+MaxPool2d	1	16	ReLU	0.1
Conv2d+MaxPool2d	16	32	ReLU	0.1
Conv2d+AdAvgPool2d	32	64	ReLU	0.1
Linear	64	2	Softmax	-
BASELINE				
Layer	In CH	Out CH	Activation	Dropout
Conv2d+MaxPool2d	1	32	ReLU	0.1
Conv2d+MaxPool2d	32	64	ReLU	0.1
Conv2d+MaxPool2d	64	128	ReLU	0.1
Conv2d+AdAvgPool2d	128	256	ReLU	0.1
Linear	256	2	Softmax	-
HEAVY				
Layer	In CH	Out CH	Activation	Dropout
Conv2d	1	64	ReLU	0.1
Conv2d+MaxPool2d	64	64	ReLU	0.1
Conv2d	64	128	ReLU	0.1
Conv2d+MaxPool2d	128	128	ReLU	0.1
Conv2d	128	256	ReLU	0.1
Conv2d+MaxPool2d	256	256	ReLU	0.1
Conv2d+AdAvgPool2d	256	512	ReLU	0.1
Linear	512	2	Softmax	-

For all *Conv2d* layers, a 3x3 kernel with a padding of 1 is used, while the *MaxPool2d* layers employed 2x2 kernels. The *AdAvgPool2d* layers correspond to *AdaptiveAvgPool2d* with an output size of 1.

Columns *In CH* and *Out CH* represent input and output channels.

implemented in Python using the PyTorch framework. Details of the model architectures are reported in Table II, while the training hyperparameters are summarized as follows: the loss function used is *CrossEntropyLoss*, optimization is performed with the *AdamW* optimizer, the learning rate is set to 10^{-3} and each model is trained for 20 epochs.

After training, the model epoch with the highest F1-score on the validation set was selected as the final model. The validation set underwent the same pre-processing steps as the training data, except for the oversampling of the *Present* class. The trained CNN outputs a binary prediction for individual 2-second segments. Patient-level classification is then derived by aggregating predictions across all segments and recording locations. Fig. 2 displays the process of the final prediction. Each segment is first classified individually, then predictions from the same location are aggregated by a "Voter" block: if the ratio of *Present* over *Absent* exceeds the value "thr", the location is classified as *Present* by the "Location Predictor" module. This procedure is repeated for all recording locations. Finally, a "Max" block analyzes the location-level results: if at least one location is classified as *Present*, the patient is predicted to have a murmur.

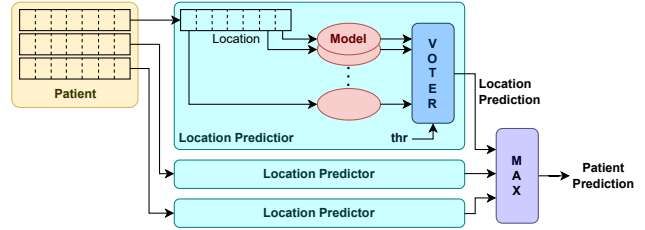


Fig. 2: Description of the patient-level prediction. An outcome is produced for each location; if at least one is positive (murmur detected) the patient is inferred to have a murmur.

The threshold "thr" is calibrated after the training phase using the validation set, with the goal of maximizing the F1-score at the location level. In the end, the same threshold value was selected for all three models, with the final value set to 40%. This value was chosen as a trade-off among the three architectures, representing an intermediate setting that balances their individual performance trends. Accordingly, the test set remains completely unseen during all stages of training and post-processing.

D. Uncertainty quantification

To estimate the reliability of the prediction of the models, MCD was applied during inference with a number of stochastic forward passes $N = 10$ [43]. For each input sample, this procedure produces N stochastic predictions in addition to the deterministic baseline output. The predictive uncertainty was then quantified using the expected entropy of the softmax outputs in the MCD samples:

$$E = - \sum p_i * \log(p_i)$$

In addition, the prediction coherence was computed:

$$C = 1 - 4 * var(p_i)$$

where p_i is the vector containing the predicted class of the 10 MCD samples. Hence, if the model always predicts the same class, $var(p_i)$ is equal to 0 and C is equal to 1. Finally, an overall confidence score (CS) is introduced that combines uncertainty and coherence as:

$$CS = \alpha * (1 - E) + (1 - \alpha) * C$$

with $\alpha = 0.5$, giving equal weight to both uncertainty and coherence. Higher values of the score indicate greater model confidence and reliability, whereas lower values correspond to uncertain or unreliable predictions.

Both uncertainty, coherence, and the overall confidence score were computed on the validation set to characterize the model behavior. The score distributions for correctly classified (CC) and misclassified (MC) samples were then analyzed to determine the decision threshold that best discriminates between the two groups.

During the inference of *Known* samples, the confidence score enabled a selective classification strategy, in which unreliable predictions (i.e., those with scores below the threshold) were discarded, resulting in improved robustness and recall. Indeed, if the ratio of confident segments was found to be less than

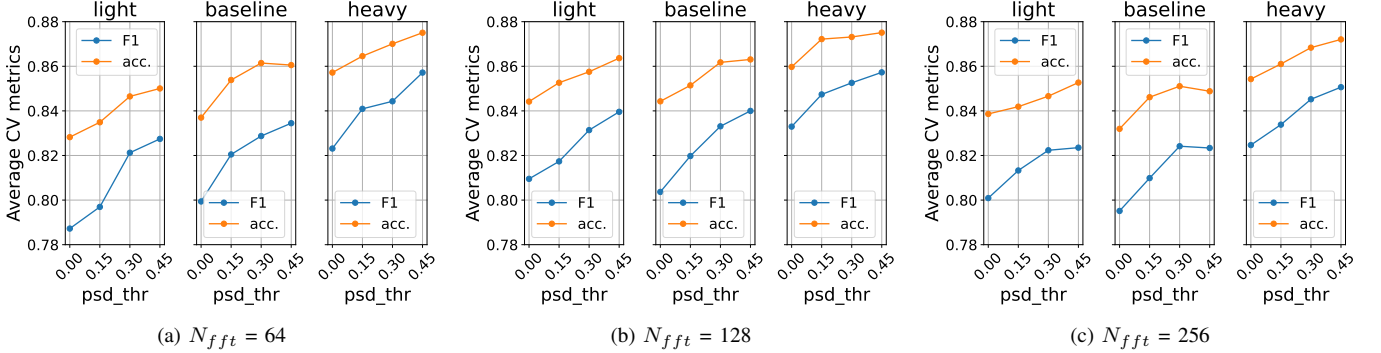


Fig. 3: Cross-validation results for the three models with N_{fft} values of 64 (a), 128 (b), and 256 (c). Each graph shows the average accuracy and F1-score across the 5 folds for different "psd_thr" values.

0.6 for a specific recording location (i.e., many segments were removed as they were considered unreliable), the threshold for determining if a specific recording contained a murmur was lowered from 40% to 20%.

Furthermore, for the *Unknown* recordings, the final confidence score provides a quantitative estimate of prediction reliability, allowing assessment of the model's behavior on clinically ambiguous cases. The Mann-Whitney statistical test was done to compare the distribution of the ratio of confident segments between the *Known* and *Unknown* recordings.

E. Evaluation metrics

Model performance was assessed using standard metrics for binary classification, considering the two classes: murmur *Present* and murmur *Absent*. Specifically, we report the classification accuracy, which measures the overall proportion of correctly classified samples, and the F1-score, defined as the harmonic mean of precision and recall, providing a balanced measure of performance in the presence of class imbalance. Precision quantifies the proportion of correctly identified positive cases among all samples predicted as positive, while the Recall (or Sensitivity) measures the proportion of correctly identified positive cases among all actual positives. These metrics were computed at the location level and then aggregated to assess overall model performance on a patient-level basis.

IV. RESULTS

A. Model performance

The impact of the N_{FFT} and psd_thr parameters was evaluated using a 5-fold cross-validation (CV) procedure. To ensure a realistic validation scenario, the folds were created at the patient level. Specifically, the 874 labeled *Absent* or *Present* patients in the training set were randomly divided into five folds, and in each iteration, the model was trained on four folds and evaluated on the remaining one. This patient-level split prevents data leakage by ensuring that segments from the same patient do not appear in both the training and validation sets, which could otherwise bias the CV results.

Three values of N_{FFT} (64, 128, and 256) were considered.

These values were selected because, given the relatively low sampling rate, increasing the FFT window beyond 256 does not improve spectrogram quality, while reducing it below 64 significantly degrades spectral resolution. Regarding the second parameter, the maximum PSD threshold tested was 0.45. Higher thresholds were not considered, as they would result in excessive segment rejection, potentially compromising the subsequent aggregation step. The CV results are reported

TABLE III: Metrics on the test set for the three final models

Model	Accuracy	F1-score	Precision	Recall
Patient-level classification employing all segments				
Light	91.18%	80.20%	80.61%	79.80%
Baseline	90.95%	79.59%	80.41%	78.79%
Heavy	90.50%	79.21%	77.67%	80.81%
Patient-level classification employing confident segments				
Light	91.40%	81.19%	79.61%	82.83%
Baseline	91.16%	80.20%	79.80%	80.61%
Heavy	90.70%	78.53%	81.52%	75.76%

in Fig. 3, which shows the average F1-score and accuracy across all folds. It is important to note that these metrics refer exclusively to segment-level classification, without including the final patient-level aggregation.

Based on the CV results, the parameters $N_{FFT} = 128$ and $psd_thr = 0.45$ were selected for the final models, as they obtain the better F1-score. Three CNN variants were then trained on the full training dataset following the complete pipeline to generate patient-level predictions. The overall performance metrics are summarized in Table III.

B. Trade-off between accuracy and model complexity

An evaluation of model complexity and size was performed with a view toward future on-the-edge deployment in embedded systems. For this purpose, the *ST Edge AI Developer Cloud* [44] online tool, developed by STMicroelectronics, was used to analyze the three proposed CNN models. The analysis focused on memory requirements (both FLASH and RAM) and the total number of multiply-and-accumulate operations (MACCs). To estimate latency, the tool provides several reference development boards on which model execution can be profiled. Three NUCLEO boards embedding MCUs with

different performance classes were selected for this evaluation. Their maximum clock frequency, FLASH memory, and RAM capacities are summarized below:

- **H743ZI2**: 480 MHz, FLASH 2MB, RAM 1MB
- **G474RE**: 170 MHz, FLASH 128 KB, RAM 512 KB
- **F401RE**: 84 MHz, FLASH 96 KB, RAM 512 KB

Additionally, the tool includes a quantization procedure that converts network weights from 32-bit floating point (float32) to 8-bit integers (int8), reducing the model size by approximately a factor of four and lowering inference latency due to faster integer operations. The results of this analysis are summarized in Table IV.

TABLE IV: Resources evaluation for the three models

	Native			Quantized		
	Light	Base	Heavy	Light	Base	Heavy
Params	23k	388k	2.33M	23k	388k	2.33M
FLASH	91KB	1.5MB	9.1MB	23KB	381KB	2.3MB
RAM	98KB	189KB	1.1MB	29KB	53KB	306KB
MACC	10.0M	56.2M	665.5M	9.9M	56.0M	664.6M
Latency						
H743ZI2	105ms	545ms	—	24ms	104ms	—
G474RE	593ms	—	—	121ms	—	—
F401RE	—	—	—	230ms	—	—

The “—” symbol indicates that the board resources are insufficient.

Quantized model results are reported in the second part of Table IV. Beyond memory reduction, quantization reduces inference latency by more than 4x. This optimization is essential for future on-the-edge deployments, where additional tasks such as signal acquisition and feature extraction will also need to be executed on the same device.

TABLE V: Metrics for the three final models quantized

Model	Accuracy	F1-score	Precision	Recall
Light	91.63%	80.63%	83.70%	77.78%
Baseline	92.08%	81.28%	86.36%	76.77%
Heavy	92.99%	83.42%	88.64%	78.79%

C. Uncertainty and confidence score analysis

Figure 4 shows the distribution of the final confidence scores of the *Known* recordings, differentiating between the correctly classified (CC) and misclassified (MC) predictions at a single segment level.

From this figure, the threshold to determine if the model was confident in the prediction of a single segment was set equal to 0.8. This resulted in removing approximately 20% of the segments on the test set. Ten independent location recordings were removed due to this pruning, but no patient was removed (i.e., no patient presented only uncertain predictions over all segments and locations).

Retaining only the segments with confident predictions resulted in performance enhancement, specifically in terms of the model Sensitivity. The bottom section of Table III portrays the same patient-level metrics for the three final models obtained when retaining only the confident segments.

Finally, the difference between the ratio of confident segments of the *Known* patients compared to the *Unknown* was done. Figure 5 portrays the results obtained on all three networks,

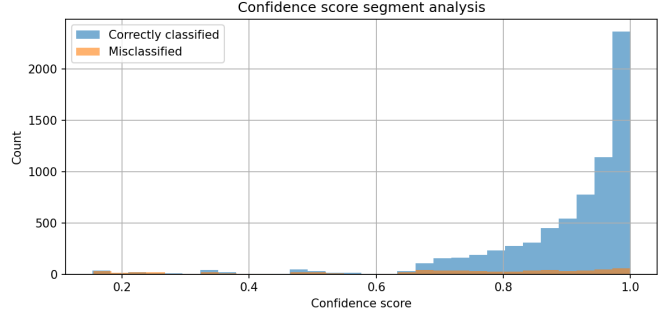


Fig. 4: Distribution of the confidence score obtained on correctly classified (CC) and misclassified (MC) samples on the *Known* samples for the Light network.

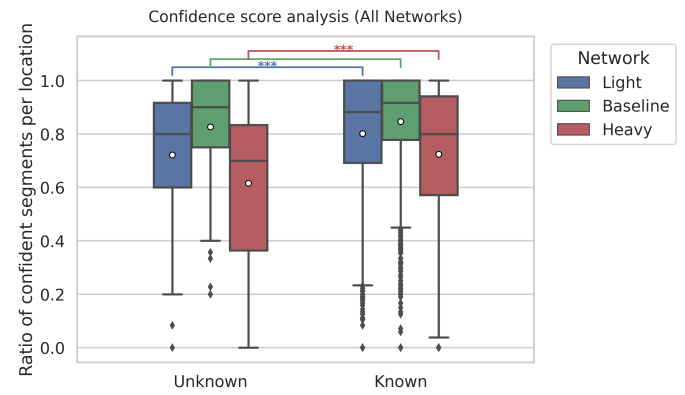


Fig. 5: Uncertainty quantification on the test set comparing the ratio of confident segments between the *Known* and *Unknown* murmur status for all three networks.

where it can be appreciated that a statistically significant difference is found for the Light and the Heavy networks.

V. DISCUSSION & CONCLUSIONS

A. Feasibility of accurate murmurs detection on the edge

The main effort of this work is to propose a method that achieves an optimal balance between detection accuracy and sensitivity and computational cost. Developing a lightweight solution is essential to enable deployment on the edge, which is a known limitation of many AI-based systems.

In our analysis, we compared three different models with three different levels of complexity. The results in Table IV clearly demonstrate the significant resource savings achieved by the Light model, particularly in FLASH memory usage, which is reduced by a factor of 102x and 17x when compared to the Heavy and Baseline models, respectively. The Heavy model cannot be deployed on any of the selected boards, highlighting the challenges of implementing large networks on hardware-constrained devices. However, as shown in Table III, the Light model exhibits comparable performance compared to the Heavy and Baseline variant, representing an excellent trade-off between predictive performance and model complexity. Furthermore, including the uncertainty quantification and confidence score selective classification, the Light model presents the best classification results and the highest sensitivity.

The use of quantization further enhances the model’s edge deployability without negatively impacting its performance: as reported in Table V, quantization has a negligible impact on prediction performance. In particular, all models suffer from a lower Recall value when employing the quantized models, favoring a higher Precision when compared to their native (float32) counterparts. Still, for on-the-edge implementation, the combination of the Light model and quantization represents the optimal solution, providing significant advantages in terms of memory and latency with a minimal sacrifice on predictive performance.

We then compared our trade-off model (Light model with quantization) with state-of-the-art cardiac murmurs classifiers. Table VI proposes a summary of existing approaches aiming for a lightweight implementation using the CirCor Digiscope dataset.

TABLE VI: Comparison against existing heart murmurs classifiers using CirCor.

Reference	Features	Classifier	Accuracy	Params
Niizumi [34]	1D segm	Transformer	83.2%	85.4M
Han [26]	Mel STFT	CNN	85.9%	141.5k
McDonald [17]	STFT	RNN+HSMM	77.6%	N/A
Kalimuthu [29]	MFCC	CNN+attention	95.2%	N/A
Guan [21]	STFT	CRNN	92.4%	43.6M
Safdar [28]	Multimodal	CNN	99.9%	2.25M
Fakhry [20]	CWT	CNN+LSTM	90.2%	3.4M
Morshed [32]	1D segm	CNN	92.2%	N/A
Ours (Light)	STFT	CNN	91.6%	23k

Our proposed trade-off model, achieving an accuracy of 91%, is in line with the state of the art. Nevertheless, it reduces the number of parameters by 2 to 4 orders of magnitude with respect to existing approaches, showing that an accurate detection is feasible even without relying on high-performance computers. Overall, the proposed pipeline for feature extraction, model training, and patient-level aggregation demonstrates a robust methodology for murmur detection, with performance that remains stable and reliable regardless of the individual model variant and in line with the best performing state-of-the-art approaches.

B. The role of uncertainty quantification

The integration of uncertainty estimation through MCD and the proposed confidence score demonstrated a positive impact on the robustness and sensitivity of the murmur detection. The application of selective classification based on the uncertainty threshold led to an increase in Recall (+3%), while the overall accuracy remained substantially unchanged. In clinical terms, this implies a reduction in missed murmur detections, that is a desirable outcome in screening applications where sensitivity is more critical than overall accuracy. This increase in Sensitivity is particularly crucial when considering how this selective classification can in the future be effectively employed on edge solutions.

Furthermore, the uncertainty analysis on the confidence score observed in the boxplots (Fig. 5) revealed significantly lower confidence scores for the unknown test samples, especially in the Light and Heavy models. This trend mirrors the

diagnostic uncertainty observed among clinical experts for the same recordings, suggesting that the model’s uncertainty estimates are meaningful and aligned with human diagnostic confidence. Such behavior reinforces the potential of UQ as a complementary tool for interpretable and trustworthy AI-based auscultation, capable of supporting non-expert users in low-resource settings.

C. Limitations and assumptions

Despite the promising results, several limitations should be acknowledged. First, the study was conducted exclusively on the CirCor dataset considering the binary murmur detection. The dataset, although large and diverse, represents a specific pediatric population and acquisition setting. This limits the generalizability of the results to other age groups, recording devices, and environmental conditions. Moreover, the dataset annotations inherently contain label noise, particularly for the *Unknown* class, which may affect both training and evaluation reliability. Secondly, the proposed uncertainty quantification relies on Monte Carlo Dropout, which provides a practical yet approximate Bayesian estimation. Other sources of epistemic and aleatoric uncertainty, such as model architecture variability or sensor noise, were not explicitly modeled. In addition, although the edge-deployment feasibility was assessed through simulation tools, real on-board testing was not performed. Therefore, latency and energy consumption measurements are only indicative.

D. Potential future directions

Future research will focus on extending the present framework along several directions. First, model generalization will be evaluated through external validation on independent datasets and recordings acquired with different stethoscope hardware and using wearable multi-sensor arrays, to assess robustness to domain shift and recording variability. From a system perspective, full edge deployment will be pursued through firmware integration and testing on embedded hardware prototypes, including real-time audio preprocessing and inference. Furthermore, explainability techniques, such as saliency or relevance mapping, could be combined with uncertainty quantification to provide clinicians and non-expert users with interpretable visual feedback.

REFERENCES

- [1] W. H. Organization, “Global health estimates: Leading causes of death. cause-specific mortality, 2000–2021.”
- [2] M. Sharma, R. John, S. Afrin, X. Zhang, T. Wang, M. Tian, K. S. Sahu, R. Mash, D. Praveen, and K. Saif-Ur-Rahman, “Cost-effectiveness of population screening programs for cardiovascular diseases and diabetes in low-and middle-income countries: a systematic review,” *Frontiers in public health*, vol. 10, p. 820750, 2022.
- [3] S. Ainsworth, J. P. Wyllie, and C. Wren, “Prevalence and clinical significance of cardiac murmurs in neonates,” *Archives of Disease in Childhood - Fetal and Neonatal Edition*, vol. 80, no. 1, pp. F43–F45, 1999.
- [4] J. W. Newburger, A. Rosenthal, R. G. Williams, K. Fellows, and O. S. Miettinen, “Noninvasive tests in the initial evaluation of heart murmurs in children,” *The New England Journal of Medicine*, vol. 308, no. 2, pp. 61–64, 1983.

[5] A. K. Ewer, L. J. Middleton, A. T. Furmston, and PulseOx Study Group, "Pulse oximetry screening for congenital heart defects in newborn infants (pulseox): A test-accuracy study," *The Lancet*, vol. 378, no. 9793, pp. 785–794, 2011.

[6] E. Braunwald, "A textbook of cardiovascular medicine," *Examination of the patient*, 1992.

[7] J. Oliveira, F. Renna, P. Costa, M. Nogueira, A. C. Oliveira, A. Elola, C. Ferreira, A. Jorge, A. B. Rad, M. Reyna *et al.*, "The circor digiscope phonocardiogram dataset (version 1.0.3)," in *PhysioNet*, 2022.

[8] J. Oliveira, F. Renna, P. D. Costa, M. Nogueira, C. Oliveira, C. Ferreira, A. Jorge, S. Mattos, T. Hatem, T. Tavares *et al.*, "The circor digiscope dataset: from murmur detection to murmur classification," *IEEE journal of biomedical and health informatics*, vol. 26, no. 6, pp. 2524–2535, 2021.

[9] M. A. Reyna, Y. Kiarashi, A. Elola, J. Oliveira, F. Renna, A. Gu, E. A. Perez Alday, N. Sadr, A. Sharma, J. Kpodonu *et al.*, "Heart murmur detection from phonocardiogram recordings: The george b. moody physionet challenge 2022," in *medRxiv*, 2022.

[10] D. A. Adedinsewo, D. Onietan, A. C. Morales-Lara, S. Moideen Sheriff, B. B. Afolabi, O. A. Kushimo, A. C. Mbakwem, K. F. Ibiyemi, J. A. Ogunmodede, H. O. Raji *et al.*, "Contextual challenges in implementing artificial intelligence for healthcare in low-resource environments: insights from the spec-ai nigeria trial," *Frontiers in Cardiovascular Medicine*, vol. 12, p. 1516088, 2025.

[11] R. R. Dangi, A. Sharma, and V. Vageriya, "Transforming healthcare in low-resource settings with artificial intelligence: Recent developments and outcomes," *Public Health Nursing*, vol. 42, no. 2, pp. 1017–1030, 2025.

[12] M. Hartmann, U. S. Hashmi, and A. Imran, "Edge computing in smart health care systems: Review, challenges, and research directions," *Transactions on Emerging Telecommunications Technologies*, vol. 33, no. 3, p. e3710, 2022.

[13] C. Guo, G. Pleiss, Y. Sun, and K. Q. Weinberger, "On calibration of modern neural networks," 2017.

[14] S. Seoni, V. Jahmunah, M. Salvi, P. D. Barua, F. Molinari, and U. R. Acharya, "Application of uncertainty quantification to artificial intelligence in healthcare: A review of last decade (2013–2023)," *Computers in Biology and Medicine*, vol. 165, p. 107441, 2023.

[15] H. Asgharnezhad, A. Shamsi, R. Alizadehsani, A. Khosravi, S. Navavandi, Z. A. Sani, D. Srinivasan, and S. M. S. Islam, "Objective evaluation of deep uncertainty predictions for COVID-19 detection," *Scientific reports*, vol. 12, no. 1, p. 815, Jan. 2022.

[16] Y. Geifman and R. El-Yaniv, "Selective classification for deep neural networks," 2017.

[17] A. McDonald, M. J. Gales, and A. Agarwal, "A recurrent neural network and parallel hidden markov model algorithm to segment and detect heart murmurs in phonocardiograms," *medRxiv*, 2023.

[18] Y. Xu, X. Bao, H.-K. Lam, and E. N. Kamavuako, "Hierarchical multi-scale convolutional network for murmur detection on pcg signals," in *2022 Computing in Cardiology (CinC)*, vol. 498, 2022, pp. 1–4.

[19] M. A. Reyna, Y. Kiarashi, A. Elola, J. Oliveira, F. Renna, A. Gu, E. A. Perez Alday, N. Sadr, A. Sharma, J. Kpodonu *et al.*, "Heart murmur detection from phonocardiogram recordings: The george b. moody physionet challenge 2022," *PLOS Digital Health*, vol. 2, no. 9, p. e0000324, 2023.

[20] M. Fakhry and A. Gallardo-Antolín, "A hybrid neural network with multistage feature fusion for detecting heart failure and murmurs from time-frequency representations of phonocardiograms," *Systems and Soft Computing*, p. 200391, 2025.

[21] T. Guan, Z. Chen, D. Xu, M. Zeng, C. Zuo, X. Wang, S. Cai, J. Wang, and N. Hu, "Lachest: An ai-assisted auscultation tool for pediatric congenital heart diseases screening and validated via large-scale screening tasks," *Biomedical Signal Processing and Control*, vol. 103, p. 107474, 2025.

[22] L. Orozco-Reyes, M. A. Alonso-Arévalo, E. García-Canseco, R. F. Ibarra-Hernández, and R. Conte-Galván, "A deep-learning approach to heart sound classification based on combined time-frequency representations," *Technologies*, vol. 13, no. 4, p. 147, 2025.

[23] I. Fernando, D. Kannangara, S. Kodituwakklu, A. Sirithunga, S. Gayan, T. Herath, N. Lokunarangoda, and R. Liyanaarachchi, "Machine learning based heart murmur detection and classification," *Biomedical Physics & Engineering Express*, vol. 11, no. 1, p. 015052, 2024.

[24] A. Patwa, M. M. U. Rahman, and T. Y. Al-Naffouri, "Heart murmur and abnormal peg detection via wavelet scattering transform & a 1d-cnn," *IEEE Sensors Journal*, 2025.

[25] A. McDonald, M. J. Gales, and A. Agarwal, "A recurrent neural network and parallel hidden markov model algorithm to segment and detect heart murmurs in phonocardiograms," *PLOS Digital Health*, vol. 3, no. 11, p. e0000436, 2024.

[26] S. Han, T. Kang, J. Lee, N. Kim, H. Won, Y.-H. Kim, W. Gong, and I.-Y. Kwak, "A deep neural network approach to heart murmur detection using spectrogram and peak interval features," *Engineering Applications of Artificial Intelligence*, vol. 137, p. 109156, 2024.

[27] D. Vimalajeewa, C. Lee, and B. Vidakovic, "Multiscale analysis of heart sound signals in the wavelet domain for heart murmur detection," *Scientific Reports*, vol. 15, no. 1, p. 10315, 2025.

[28] Z. Safdar, J. Sheng, M. U. Saeed, M. Ramzan, and A. Al-Zubaidi, "Empowering cardiovascular diagnostics with set-mobilenet: A lightweight and accurate deep learning based classification approach," *Image and Vision Computing*, p. 105684, 2025.

[29] M. Kalimuthu and C. Hemanth, "A comparative analysis of machine learning and deep learning approaches for phonocardiogram classification using dataset integration," *IEEE Access*, 2025.

[30] F. Özcan, "Rapid detection and interpretation of heart murmurs using phonocardiograms, transfer learning and explainable artificial intelligence," *Health Information Science and Systems*, vol. 12, no. 1, p. 43, 2024.

[31] Y. Luo, Z. Fu, Y. Ding, X. Chen, and K. Ding, "Phonocardiogram (pcg) murmur detection based on the mean teacher method," *Sensors*, vol. 24, no. 20, p. 6646, 2024.

[32] M. Morshed and S. A. Fattah, "Deep learning based murmur detection from pcg signals collected at four valve locations using joint optimization and decision fusion," *Results in Engineering*, p. 107375, 2025.

[33] J.-M. Shin, S. Park, K. Shin, W.-Y. Seo, H.-S. Kim, D.-K. Kim, B. Moon, S.-G. Cha, W.-J. Shin, and S.-H. Kim, "Temporal convolutional neural network-based feature extraction and asynchronous channel information fusion method for heart abnormality detection in phonocardiograms," *Computer Methods and Programs in Biomedicine*, p. 108871, 2025.

[34] D. Niizumi, D. Takeuchi, Y. Ohishi, N. Harada, and K. Kashino, "Exploring pre-trained general-purpose audio representations for heart murmur detection," in *2024 46th Annual International Conference of the IEEE Engineering in Medicine and Biology Society (EMBC)*. IEEE, 2024, pp. 1–4.

[35] S. KV, D. B. Koppad, D. Raghavan, and M. PR, "Lightcardiacnet: lightweight deep ensemble network with attention mechanism for cardiac sound classification," *Systems Science & Control Engineering*, vol. 12, no. 1, p. 2420912, 2024.

[36] A. Pal, A. Roy, and U. Satija, "A unified joint contrastive triplet loss with temporal and frequency signal fusion for diagnosing heart murmurs," in *ICASSP 2025-2025 IEEE International Conference on Acoustics, Speech and Signal Processing (ICASSP)*. IEEE, 2025, pp. 1–5.

[37] M. Alkhodari, L. J. Hadjileontiadis, and A. H. Khandoker, "Identification of congenital valvular murmurs in young patients using deep learning-based attention transformers and phonocardiograms," *IEEE Journal of Biomedical and Health Informatics*, vol. 28, no. 4, pp. 1803–1814, 2024.

[38] S. Manjusree, J. D. Beegum, N. Muhsina, and P. Lubaiib, "Heart sound analysis and murmur classification using bark scale modulation spectrogram features," in *2024 2nd International Conference on Self Sustainable Artificial Intelligence Systems (ICSSAS)*. IEEE, 2024, pp. 451–458.

[39] E. Bondareva, T. Xia, J. Han, and C. Mascolo, "Towards uncertainty-aware murmur detection in heart sounds via tandem learning," in *2022 Computing in Cardiology (CinC)*, vol. 498. IEEE, 2022, pp. 1–4.

[40] X. Wang, F. Fan, H. Gao, S. Zhang, C. Yang, J. Li, and C. Liu, "Beat-wise uncertainty learning for murmur detection in heart sounds," in *2022 Computing in Cardiology (CinC)*, vol. 498. IEEE, 2022, pp. 1–4.

[41] Z. Zhang, T. Pang, J. Han, and B. W. Schuller, "Intelligent cardiac auscultation for murmur detection via parallel-attentive models with uncertainty estimation," in *ICASSP 2024-2024 IEEE International Conference on Acoustics, Speech and Signal Processing (ICASSP)*. IEEE, 2024, pp. 861–865.

[42] A. Elola, E. Aramendi, J. Oliveira, F. Renna, M. T. Coimbra, M. A. Reyna, R. Sameni, G. D. Clifford, and A. B. Rad, "Beyond heart murmur detection: automatic murmur grading from phonocardiogram," *IEEE journal of biomedical and health informatics*, vol. 27, no. 8, pp. 3856–3866, 2023.

[43] Y. Gal and Z. Ghahramani, "Bayesian convolutional neural networks with bernoulli approximate variational inference," 2016.

[44] STMicroelectronics. (2025) St edge ai developer cloud. Accessed: Oct. 22, 2025. [Online]. Available: <https://stm32ai.st.com/st-edge-ai-developer-cloud>